Distinct Lipid Rafts in Subdomains from Human Placental Apical Syncytiotrophoblast Membranes

Valeria Godoy · Gloria Riquelme

Abstract We report on the characteristics of raft domains in the apical membrane from human placental syncytiotrophoblast (hSTB), an epithelium responsible for maternal–fetal exchange. Previously, we described two isolated fractions of the hSTB apical membrane: a classical microvillous membrane (MVM) and a light microvillous membrane (LMVM). Detergent-resistant microdomains (DRMs) from MVM and LMVM were prepared with Triton X-100 followed by flotation in a sucrose gradient and tested by Western and dot blot with raft markers (placental alkaline phosphatase, lipid ganglioside, annexin 2) and transferrin receptor as a nonraft marker. DRMs from both fractions showed a consistent peak for these markers, except that the DRMs from MVM had no annexin 2 mark. Cholesterol depletion modified the segregation in both groups of DRMs. Our results show two distinguishable lipid raft subsets from MVM and LMVM. Additionally, we found significant differences between MVM and LMVM in cholesterol content and in expression of cytoskeletal proteins. MVM is enriched in ezrin and β-actin; in contrast, cholesterol and cytokeratin-7 are more abundant in LMVM. These differences may explain the distinct properties of the lipid raft subtypes.

V. Godoy
Departamento de Fisiología y Biofísica, Instituto de Ciencias Biomédicas, Facultad de Medicina, Universidad de Chile, Santiago, Chile

G. Riquelme (✉)
Fisiología y Biofísica, Instituto de Ciencias Biomédicas, Facultad de Medicina, Universidad de Chile, Casilla 70005 Santiago 7, Chile
e-mail: griquelm@med.uchile.cl

Keywords Lipid raft · Placenta · Apical membrane · Epithelium · Cytoskeleton · Detergent-resistant microdomain

Abbreviations

hSTB	Syncytiotrophoblast
PLAP	Alkaline phosphatase
Anx-2	Annexin A2
MVM	Classical microvillous membrane
LMVM	Light microvillous membrane
CK-7	Cytokeratin-7
htf-R	Human transferrin receptor
DRMs	Detergent-resistant membranes
mβ-CD	Methyl β-cyclodextrin

Introduction

In polarized epithelial cells, the apical and basolateral plasma membranes strongly differ in lipid and protein composition. Human placental syncytiotrophoblast (hSTB), epithelial cells lacking a paracellular route to separate maternal and fetal blood, constitute the main barrier for maternal–fetal exchange. To guarantee their function and to control material flow in one defined direction, hSTB maintain a polarized organization with two distinct (apical and basal) plasma membrane domains. Apical protein sorting and trafficking require specific signals; some of these depend on the integrity of sphingolipid/cholesterol-enriched membrane microdomains termed "lipid rafts," while others use separate transport platforms (Delacour and Jacob 2006; Ikonen 2001; Rajendran and Simons 2005; Schuck and Simons 2004). The raft hypothesis for apical protein transport was postulated over 10 years ago but is still a matter of updates and debate. At present, there are several lines of

evidence indicating that microdomains exist within the fluid bilayer of the plasma membrane and that protein association with lipid rafts may occur (Danielsen and Hansen 2003; Nguyen et al. 2006; Simons and Ikonen 1997). In placental epithelium, this is an emerging thesis that needs to be further explored (Paradela et al. 2005; Xu et al. 2006).

A definition of membrane rafts was clarified at the Keystone Symposium on Lipid Rafts and Cell Function: "Lipid rafts are small and highly dynamic membrane microdomains (10–20 nm) that are enriched in cholesterol and sphingolipids that compartmentalize cellular processes. Small rafts can sometimes be stabilized to form larger platforms through protein–protein and protein–lipid interactions" (Pike 2006). This arrangement makes them membrane regions with distinct properties and structural composition. They appear to act as platforms to colocalize proteins implicated in processes as diverse as signal transduction, endocytosis and cholesterol trafficking. New evidence suggests that this variety of functions is accompanied by diversity in the composition of lipid rafts. The rafts in cells appear to be heterogeneous in terms of both protein and lipid content and can be localized in separate regions of the cell (Janich and Corbeil 2007).

Different methods have been used to isolate and characterize the rafts; some of these require cellular destruction, and others are performed with live, intact cells (Lagerholm et al. 2005; Macdonald and Pike 2005). The first method to biochemically define rafts was based on their resistance to solubilization by non-ionic detergents such as Triton X-100 at 4°C (Brown and Rose 1992). The detergent-resistant membrane (DRM) fractions that result from this technique are aggregates of raft domains and thus do not represent the native state of lipid rafts in cell membranes (Lichtenberg et al. 2005). However, DRMs have proved to be a useful starting point for the analysis of microdomains (Babiychuk and Draeger 2006; Hanada et al. 1995; Schroeder et al. 1998). A large number of cell surface proteins are found in lipid rafts (Babiychuk et al. 2002; Chatterjee et al. 2001; Rajendran et al. 2003; Simons and Toomre 2000), and increasing evidence suggests that partitioning of a protein in and out of rafts could play a role in diverse pathologies (Fantini et al. 2002; Simons and Ehehalt 2002).

The apical membrane of epithelial cells, including hSTB, is a specialized structure particularly rich in membrane lipids characteristic of lipid rafts, which seem to be essential for the maintenance and stability of microvilli (Meder et al. 2006). These lipids include several raft markers, such as placental alkaline phosphatase (PLAP) and annexin 2 (Anx-2), which have been found in microvillous rafts (Hanada et al. 1995; Harder et al. 1998; Harder and Gerke 1994). Additionally, in the apical domain, a heterogeneous population of rafts in the microvillous membrane has been demonstrated (Braccia et al. 2003; Roper et al. 2000); these are probably involved in specific functions and may be linked to cytoskeletal proteins (Arvanitis et al. 2005; Crane and Tamm 2004; Schuck and Simons 2004). Given that the microdomains in human placental epithelium are still poorly understood, we set out to find and characterize rafts from purified apical membrane fractions of hSTB.

Previously, using differential sucrose density migration, we isolated two fractions from the apical (maternal-facing) membrane: the classical microvillous membrane (MVM), used by us and other authors to study transport mechanisms, and the light microvillous membrane (LMVM) (Jimenez et al. 2004). We described a Maxi chloride channel (Bernucci et al. 2003; Riquelme et al. 1995, 2004; Riquelme and Parra 1999; Vallejos and Riquelme 2007), a nonspecific cation channel in MVM (Llanos et al. 2002) and, more recently, K^+ channels in LMVM (Berrios et al. 2008; Vallejos et al. 2008), suggesting that the two fractions could contain different transport proteins. Although we reported based on mass spectrometry that MVM from hSTB is probably highly enriched in lipid raft microdomains (Paradela et al. 2005), this does not constitute direct evidence. On the other hand, LMVM has not been fully studied and we suppose that raft composition could be one factor that distinguishes it from the MVM fraction.

The aim of this work was to study the differential expression of microdomain lipid rafts in both purified apical membrane fractions of hSTB and to explore possible connections with the cytoskeleton. These studies could improve our understanding of the physiological role of these domains and their constituents.

Materials and Methods

Placenta Collection

Placentae obtained from normal pregnancies were collected immediately after delivery from the San José Hospital Maternity Unit and transported to the laboratory on ice.

Preparation of Placental Apical Membranes

Human placental apical membrane or MVM and LMVM vesicles were prepared from fresh placenta by a method we have described that enables simultaneous isolation of apical and basal membranes from the same placenta (Jimenez et al. 2004). The purification method included precipitation of non-MVM with magnesium ions, differential centrifugation and a sucrose step gradient; this assured that isolated fractions were enriched and free of contamination. All solutions were buffered with 20 mM Tris-maleate (pH 7.4).

A portion (2–3 ml) of the microvillous-enriched preparation containing about 10–15 mg of protein was overlaid on the sucrose gradient. Bands were obtained at 10/37% and 37/45% sucrose interfaces, corresponding to an LMVM apical fraction and to the classical MVM apical fraction, respectively. These fractions were collected and diluted 10-fold with 20 mM Tris-maleate (pH 7.4) before centrifugation at 110,000 × *g* for 30 min. The final pellet was resuspended in 300 mM sucrose, 20 mM Tris-maleate (pH 7.4) buffer and stored in liquid nitrogen. Protein concentration was determined using a bicinchoninic acid (BCA) protein assay kit (Pierce Biotechnology, Rockford, IL, USA) for the colorimetric detection and quantification of total protein (Smith et al. 1985; Wiechelman et al. 1988). The purity and enrichment of the fractions were determined routinely by assaying for alkaline phosphatase activity, an apical membrane marker; adenylate cyclase, a basal membrane marker; and cytochrome-*c* oxidase and succinate dehydrogenase, mitochondrial membrane markers. Enrichment of alkaline phosphatase activity was over 20-fold for MVM and LMVM; both preparations were essentially free of basal membranes and mitochondrial membranes. The purity and cross-contamination of the membranes were similar to those previously observed (Jimenez et al. 2004).

Preparation of Apical Lipid Microdomains

Apical plasma membrane microdomains were isolated from MVM and LMVM enriched membrane fractions separately as a DRM through extraction with Triton X-100 using a modified protocol based on that described by Brown and Rose (1992). Briefly, aliquots of 0.6 mg of both isolated membrane fractions were homogenized 30 times in a manual glass homogenizer with 1% Triton X-100 in MBS-buffered saline (25 mm morpholinoethanesulfonic acid [MES], 150 mm NaCl, pH 6.5). After 90 min incubation on ice, 1 ml of vesicles from both apical fractions (MVM and LMVM) was mixed with 1 ml of 80% sucrose to obtain a final sucrose concentration of 40%. Then, a discontinuous gradient was prepared by overlaying the 40% cushion with 2 ml of 35% sucrose and 1 ml of 5% sucrose in an AH-650 Sorvall (Wilmington, DE, USA) tube. All sucrose solutions were made in MBS (pH 6.5). The tubes were centrifuged at 21,700 × *g* for 20–22 h. After centrifugation, the gradients were divided into 10 fractions (0.5 ml each) from the top of the gradient; the pellet was resuspended in 0.5 ml MBS (fraction 11) for subsequent analysis. Throughout this article, we use the term "lipid microdomains" or "DRMs" as the membrane material that floats on the sucrose gradient around the 5/35% interface (fractions 1–5).

Characterization of Apical Membrane Flotation Gradient Fractions

All flotation fractions from MVM and LMVM were characterized by specific markers for protein or lipid content, alkaline phosphatase as a positive marker for apical lipid microdomain fractions and human transferrin receptor (htf-R) as a nonraft marker. Additionally, we used another raft marker protein, Anx-2, and a lipid marker, glycosphingolipid (GM1) (Babiychuk and Draeger 2000; Danielsen and Hansen 2003; Gaus et al. 2005; Harder and Gerke 1994; van der Goot and Harder 2001).

Depletion of Membrane Cholesterol by Methyl-β-Cyclodextrin Treatment

Cyclodextrin treatment was carried out as described previously (Danielsen and Hansen 2003). Placental apical vesicles (0.6 mg of total protein) were incubated with 2% w/v methyl-β-cyclodextrin (mβ-CD) in MBS buffer at 37°C for 30 min and centrifuged at 21,000 × *g* for 2 h at 4°C. The pellet was resuspended in 1 ml of 1% Triton X-100 in MBS, and the microdomain preparation was carried out as described above.

Electrophoresis, Western Blotting and Densitometric Analysis

All flotation gradient fractions were tested by SDS-PAGE and immunoblotting. Aliquots of 50 µl each were incubated with 10% trichloroacetic acid (v/v) for 30 min on ice and centrifuged at 21,000 x *g* for 30 min at 4°C. The pellet was resuspended in sample buffer, boiled for 5 min and sonicated for 30 min. For the cytoskeletal proteins ezrin, cytokeratin-7 (CK-7) and β-actin, 20 µg of total protein of LMVM and MVM was used; routinely all three proteins had been probed in membrane fractions isolated from the same placentae. These samples and the molecular weight marker (Dual Colour; Bio-Rad, Richmond, CA, USA) were loaded on a 10% SDS-polyacrylamide gel. Electrophoresis was performed at 100 *V,* and the gel was transferred to a nitrocellulose membrane (Bio-Rad 162-0115) for 2 h at 100 *V*. The nitrocellulose membrane was blocked for 2 h at room temperature with 3% nonfat milk in Tween/saline buffer (138 mM NaCl, 270 mM KCl, 0.05% Tween-20) and washed in Tween/saline buffer. Membranes were incubated with primary antibody for 2 h at room temperature. All antibodies were diluted in distilled water: anti-PLAP 1:5,000, anti-Anx-2 1:2,000, anti-htf-R 1:500, anti-ezrin 1:2,000, anti-CK-7 1:500, anti-β-actin 1:5,000. After washing with Tween/saline buffer, membranes were incubated with specific horseradish peroxidase (HRP)–linked secondary antibody: anti-rabbit 1:5,000 or anti-mouse

1:10,000, both diluted in Tween/saline buffer and incubated for 1 h at room temperature. Bands were detected with the enhanced chemiluminescence Western Blotting Analysis System (ECL, RPN 2106; Amersham, Arlington Heights, IL, USA). Protein content was quantified with UN-SCAN-IT gel Automated Digitizing System, version 4.1 (Silk Scientific, Orem, UT).

Dot Blotting

To measure the expressions levels of GM1 in each fraction, 3 µl of flotation gradient fractions were dot-blotted on nitrocellulose membrane, dried for 1 h and blocked for 2 h with 3% BSA in PBS (128 mM NaCl, 2 mM KCl, 8 mM Na_2HPO_4, 2 mM K_2HPO_4, pH 7.2) at room temperature. Later, the membrane was incubated overnight with the HRP-conjugated cholera toxin β-subunit (1:10,000) and detected with the ECL system. Densitometric analysis of dot-blot bands was performed in the UN-SCAN-IT gel 4.1 system.

Reagents and Antibodies

All chemicals were analytical grade. Buffers were made with distilled water, and pH values were determined at room temperature. The following antibodies were used: mouse monoclonal antibody to human PLAP (Sigma, St. Louis, MO), β-actin (MP Biomedicals, Santa Ana, CA), ezrin (Zymed, San Francisco, Ca), CK-7 (Zymed), htf-R (Zymed), rabbit polyclonal antibody to Anx-2 (Santa Cruz Biotechnology, Santa Cruz, CA) and HRP-conjugated secondary goat anti-mouse (Amersham) and rabbit (Santa Cruz Biotechnology). For dot blotting to GM1, HRP-conjugated cholera toxin β-subunit (Sigma) was used.

Statistical Analysis

Results are expressed as the mean ± sem. Measures of statistical significance were obtained using Student's *t*-test. $P < 0.05$ was considered significant.

Results

hSTB Apical Domain Characterization

Purification of apical membrane fractions (MVM and LMVM) from placental hSTB was achieved using the protocol described in "Materials and Methods," which resulted in adequate enrichment of apical membrane markers essentially free of basal membranes and mitochondrial membranes, as described fully in a previous report (Jimenez et al. 2004).

Microvillous enrichment was assessed using the enzymatic activity of PLAP, an epithelial apical membrane marker that is abundant in the syncytiotrophoblast microvillous membranes but scarce or absent in other cell membranes in the human placenta. The enrichment factors relative to the initial tissue homogenate can be seen in Fig. 1a (PLAP enrichment activity). The alkaline phosphatase activity in pure LMVM and MVM is enriched 26.2 ± 3.9- and 21.9 ± 3.1-fold relative to the homogenate, respectively ($n = 8$ independent placentae). Similar results were obtained from Western blot analysis, demonstrating the presence of alkaline phosphatase in both LMVM and MVM fractions. An interesting result is that the enriched value for LMVM is slightly greater than that of MVM. The enrichment activity of the purified apical membrane fractions was comparable to those of other preparations reported for apical membrane purification (Jimenez et al. 2004).

Since cholesterol is known to be enriched in rafts and is critical to their formation, our first approach was to measure cholesterol content in the two apical fractions. Total cholesterol was estimated in the apical fractions using an enzymatic assay described in "Materials and Methods." As shown in Fig. 1b, the cholesterol/protein ratio of LMVM (0.25 ± 0.03) was considerably higher (1.7-fold) than the MVM ratio (0.15 ± 0.01, $n = 6$ placentae).

Presence of Lipid Microdomains in the Apical Fractions of hSTB

We implemented a protocol to obtain DRMs from LMVM and MVM. Placental apical membranes were incubated with 1% Triton X-100, layered in a discontinuous sucrose gradient (5–35–40%), centrifuged for 20–22 hr until separation occurred and collected in 10 fractions of 0.5 ml, of which fractions 1–5 were considered DRMs; the pellet was resuspended as fraction 11.

First, all fractions were probed for PLAP, a recognized apical and raft marker. Figure 2a shows the distribution of this marker in the flotation gradient fractions. PLAP is enriched in DRMs from LMVM, specifically in fraction 3 (27.6 ± 3.6), which corresponds to the 5–35% interface. A previous report found this level of the gradient to be where the main rafts float (Brown and Rose 1992). Fraction 3 also had significantly more PLAP than the rest of the fractions ($n = 6$ placentae). For MVM, two important peaks were observed for PLAP: the first corresponding to the DRM fractions (14.2 ± 4.7), the second (23.7 ± 2.5) corresponding to the pellet ($n = 6$ placentae), which has greater enrichment of this marker. Although both apical membranes showed a PLAP peak in the DRM fractions, suggesting the presence of rafts in both membranes, there were differences between them. PLAP was higher in

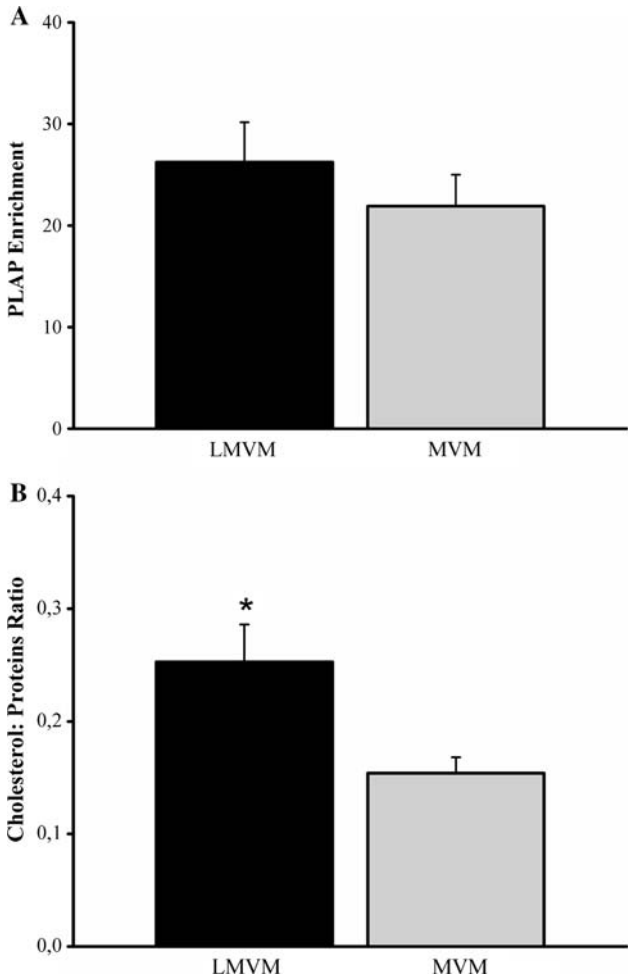

Fig. 1 Characteristics of apical hSTB domains. (**a**) Enrichment of PLAP activity in LMVM and MVM. Enrichment values (26.2 ± 3.9 and 21.9 ± 3.1, respectively) indicate that both fractions came from the apical domain of hSTB ($n = 8$ placentae). (**b**) Graph shows cholesterol content in each apical fraction normalized as cholesterol/protein ratio. LMVM has significantly higher cholesterol content (0.25 ± 0.03) compared to the MVM fraction (0.15 ± 0.01) ($n = 6$ placentae, mean ± sem, $^*P < 0.05$)

LMVM DRMs than in the corresponding fractions from MVM, while in the pellets PLAP was higher in MVM than in LMVM.

In addition, to ensure that the DRM fractions were free of nonraft fractions, which could correspond to poorly solubilized complexes from the weak detergent treatment, we probed these fractions for htf-R, a protein known to reside in nonraft areas. As Fig. 2a shows, this protein is not found in DRM fractions from LMVM or MVM ($n = 4$ placentae).

Characterization of DRMs from LMVM and MVM

DRM fractions were further assayed for two membrane compounds known to be enriched in the Triton X-100-insoluble rafts: GM1, a glycosphingolipid marker, and Anx-2, a protein associated with cholesterol and cytoskeleton and linked to the cytoplasmic side of the membrane. Figure 3a shows the distribution of Anx-2 in the LMVM and MVM flotation gradient fractions. This marker appeared in a small peak in the DRM fractions of LMVM, and the main mark (~90%) appeared in the soluble fractions, including the pellet fraction. By contrast, in the MVM flotation fractions, Anx-2 was totally absent in the DRMs and all of the marks (100%) appeared in the nonraft fractions. On the other hand, GM1 (Fig. 3b) showed a similar distribution pattern to PLAP for both LMVM and MVM. In LMVM, GM1 showed a unique peak of enrichment (26.4 ± 2.0) in the DRM fractions. In MVM flotation gradient fractions, GM1 was present in two peaks: the first of these corresponding to DRM fractions (10.8 ± 4.7), significantly less than that in LMVM, and the second corresponding to the pellet (37.8 ± 3.5), higher than that in LMVM.

Cholesterol-Depletion Effects on the Distribution of Raft Markers

Cholesterol depletion has been shown to directly affect protein association with rafts and inhibit raft-dependent signaling. Therefore, to establish a relationship between cholesterol content and raft marker association, we removed cholesterol from LMVM and MVM membranes by treating them with mβ-CD, a specific cholesterol removal agent. Apical membranes were incubated with 2% mβ-CD as described in "Materials and Methods." This resulted in 95% depletion of membrane cholesterol as judged by comparing cholesterol/protein ratios before and after treatment (data not shown). As has been reported in the literature, cholesterol depletion affects the association of various raft markers with the DRM fractions in different ways. As shown in Fig. 4, PLAP association with DRM fractions from LMVM and MVM was not affected by removal of cholesterol. GM1 association, however, was significantly decreased by 2% mβ-CD treatment. The GM1 signal fell from 64.2 ± 5.5 to 42.8 ± 5.5 in the LMVM DRMs and from 24.6 ± 5.3 to 4.2 ± 2.2 in MVM ($n = 6$ control placentae, $n = 4$ mβ-CD preincubated placentae). Anx-2, present only in the DRM fractions of LMVM, was completely absent after cholesterol extraction, suggesting that this association depends directly on the presence of cholesterol in LMVM.

Possible Cytoskeletal Participation in Differential Composition of Rafts

Based on the results described above, the next step was to test the specialized cytoskeleton. The cytoskeleton stabilizes the microvilli of the syncytium and may be linked to

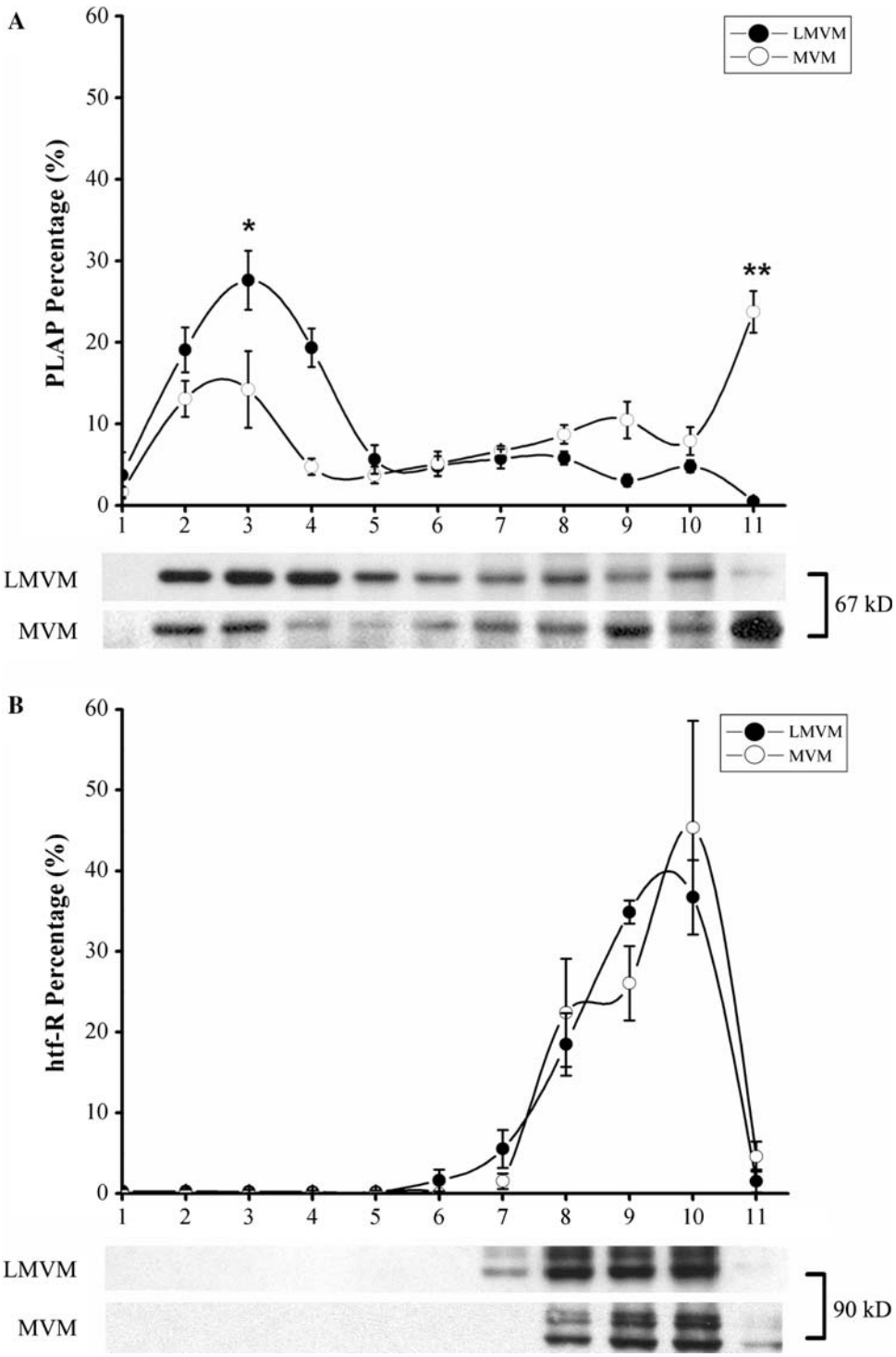

Fig. 2 Distribution of raft and nonraft markers in the flotation gradient fractions of LMVM and MVM. Equal volumes of each sucrose gradient fraction of LMVM and MVM were separated by SDS-PAGE, transferred to a nitrocellulose membrane and probed for PLAP, a typical raft marker, and for htf-R, a nonraft marker. The amount shown is expressed as a percentage of the sum of all fractions. (**a**) Representative image and quantification of Western blot analysis of PLAP shows a peak between fractions 1 and 5 corresponding to DRMs of both LMVM and MVM ($n = 6$ placentae, mean ± sem, $^{*}P < 0.05$ and $^{**}P < 0.01$). (**b**) Representative image and quantification of Western blot analysis of htf-R show that it is absent from DRM fractions in both LMVM and MVM membranes ($n = 4$ placentae, mean ± sem)

the differential distribution of raft markers between the two apical membrane fractions of hSTB. LMVM and MVM were analyzed for three cytoskeletal proteins, ezrin, β-actin and CK-7, which are localized in different parts of the cytoskeletal apical domain (Berryman et al. 1995; Morales et al. 2004; Tyska et al. 2005; Wald et al. 2005). As Fig. 5 shows, ezrin and β-actin proteins, associated with the microvillous finger-like projection region, were significantly more associated with MVM than LMVM (65.0 ± 3.4 vs. 34.9 ± 3.7 for ezrin, 62.6 ± 3.3 vs. 37.4 ± 3.5 for β-actin). CK-7, which is a component of the intermediate filaments in whole trophoblast epithelia, was more abundant in LMVM than in MVM (66.2 ± 6.1 vs. 33.8 ± 6.0). These results suggest that LMVM could correspond to the apical subdomain constituting the base of finger-like projections, which interact with the intermediate

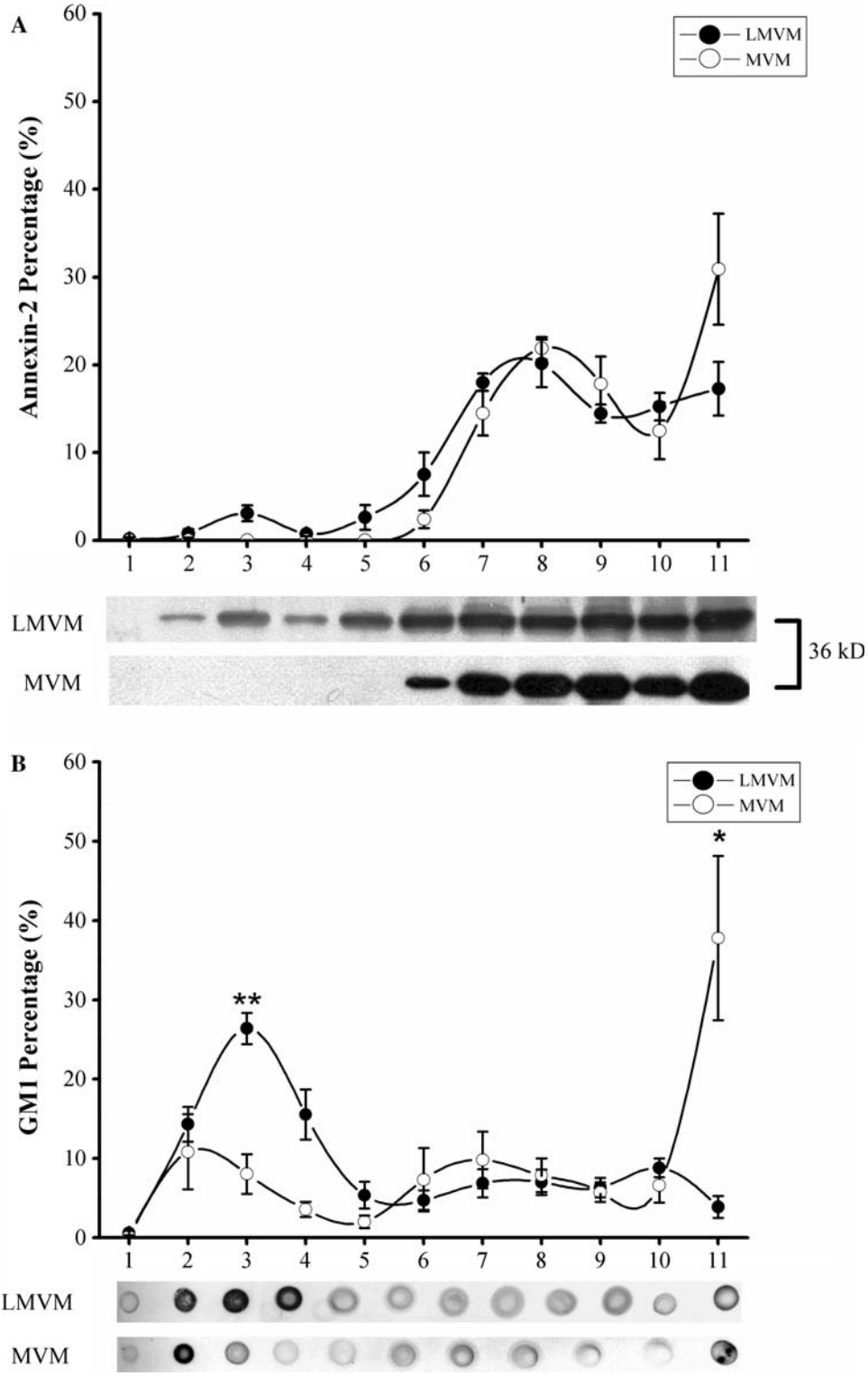

Fig. 3 Differential distribution of raft markers in the flotation gradient fractions of LMVM and MVM. (**a**) Representative image and quantification of Western blot analysis of Anx–2 show the flotation gradient fractions. No mark was detected in the DRM fractions of MVM, and only a weak mark was present in the DRM fractions of LMVM. The amount shown is expressed as a percentage of the sum of all fractions ($n = 6$ placentae, mean ± sem). (**b**) The lipid GM1 shows a unique peak in the DRM fractions of LMVM and two peaks in the flotation fractions of MVM ($n = 6$ placentae, mean ± sem, $^{*}P < 0.05$ and $^{**}P < 0.01$). A representative image of the dot blots for GM1 is in the bottom panel

filaments of the trophoblast cytoskeleton. The MVM could correspond to the microvillous finger-like region of the apical subdomain of hSTB. Thus, differences in the DRMs from the apical membranes might be explained by LMVM and MVM deriving from two distinct apical domains.

Discussion

Here, we report the differential expression of microdomains (lipid rafts) in both MVM and LMVM, purified microvillous membranes from placental hSTBs previously

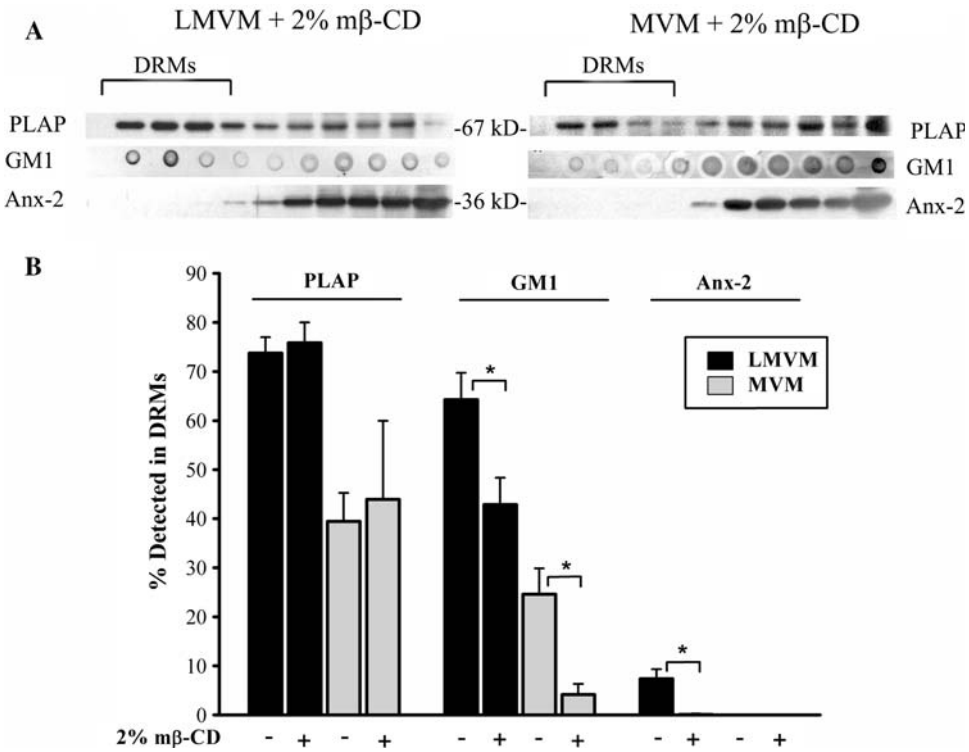

Fig. 4 Cholesterol depletion affects the association of raft markers with Triton X–100-resistant complexes. (**a**) Representative Western blot images of raft markers distributed among the flotation gradient fractions obtained from cholesterol-depleted LMVM and MVM. (**b**) Graph summarizing the cholesterol-depletion effect; the percentage shown corresponds to the sum of relative density in fractions 1–5 of each apical membrane, control and preincubated with mβ-CD. In both apical membranes GM1 was partially removed from DRMs and Anx-2 was completely removed from DRMs of LMVM. Otherwise, PLAP showed the same expression ($n = 6$ control placentae, $n = 4$ mβ-CD preincubated placentae, mean $\pm$ sem, $^*P < 0.05$)

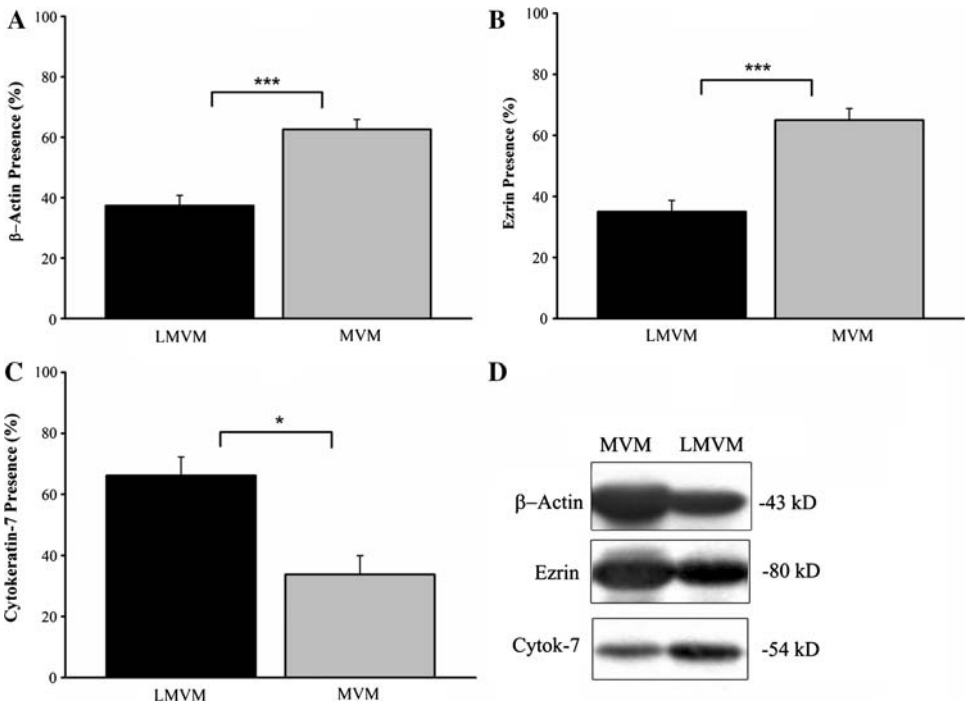

Fig. 5 Comparison of cytoskeletal proteins detected in LMVM and MVM apical membranes. Graphs (**a–c**) show the differential expression of β-actin, ezrin and CK-7, respectively. All three proteins had been probed in membrane fractions isolated from the same placentae ($n = 8$ independent placentae). The values presented as percentage correspond to relative density of the mark present in each apical fraction, which was normalized by the sum of densities in both fractions (mean $\pm$ sem, $^*P < 0.05$, $^{***}P < 0.01$). (**d**) Representative images of Western blots for cytoskeletal proteins in membrane fractions isolated from the same placenta

described by us (Jimenez et al. 2004). We show that the two apical membrane fractions have different cholesterol content and cytoskeletal protein composition including CK-7, ezrin and β-actin. These results confirm the heterogeneity of hSTB apical membrane domains, specifically their protein and lipid composition, and suggest the existence of two subdomains within the apical domains.

In both purified apical membranes we observed features of sphingolipid/cholesterol-enriched membrane microdomains characterized by their resistance to detergent

extraction and the ability to float in density gradient centrifugation. However, we obtained two different DRM fractions by Triton X-100 treatment and from samples of the 5% and 35% bands of the sucrose gradient. The analysis of sucrose density gradient fractions with three raft markers (PLAP, Anx-2 and GM1) and for htf-R, a nonraft marker (Harder et al. 1998), allowed us to distinguish between the two types of DRMs. We assayed PLAP first, obtaining an unequal distribution in MVM and LMVM, and inferred that the distinct pattern of PLAP distribution could reflect a different type of raft in each apical membrane fraction. The flotation gradient fractions were further analyzed for two membrane compounds known to be enriched in the Triton X-100-insoluble rafts: GM1 and Anx-2. In LMVM, a consistent peak of all markers was present in fractions 1-5, as expected for DRMs; however, in MVM, a heterogeneous distribution pattern of the DRM markers was observed: PLAP and GM1 were detected as expected, but Anx-2 was absent from these DRMs. htf-R, a protein known to reside in nonraft regions, was absent from LMVM and MVM DRMs, indicating that the presence of PLAP, GM1 and Anx-2 in DRMs was not due to contamination from nonraft zones. In addition, cholesterol depletion considerably altered GM1 and Anx-2 levels but had no effect on PLAP.

In conclusion, our results describe two distinguishable DRM subsets from MVM and LMVM purified apical membranes, representing the first evidence of the presence of microdomains in isolated apical syncytiotrophoblast membranes. These results agree with those of Xu et al. (2006), who described lipid rafts from a homogenate of placental tissue. In our case, the results determine the specific tissue localization (apical membrane fractions) of the lipid rafts and their differing composition, suggesting that the purified apical fractions obtained, MVM and LMVM, constitute two structurally distinct regions or subdomains in the microvillous membrane of the apical domain of hSTB.

The existence of microdomains within the fluid bilayer of the apical plasma membrane of hSTB is in agreement with several reports that describe rafts in both excitable and nonexcitable cells including epithelial cells, which localize a number of membrane proteins together with multiple signal-transduction molecules, while excluding others associated with multiple functions (Danielsen and Hansen 2003; Mazzone et al. 2006; Nguyen et al. 2006; Simons and Ikonen 1997; Taieb et al. 2004). The heterogeneity that we observed is also compatible with the literature, where marker protein assays and ultrastructural data indicate the existence of different types of rafts (Danielsen and Hansen 2003; Volonte et al. 1999). A growing body of work suggests that the variety of functions associated with lipid rafts is accompanied by diversity in their composition (Arvanitis et al. 2005; Danielsen and Hansen 2003; Janich and Corbeil 2007).

Together with two distinct raft types, a systematic second peak of raft markers in the pellet flotation fraction was found only in MVM. The next step was to explore whether the specialized cytoskeleton that stabilizes the microvilli of the syncytium could be involved in the differential distribution of raft markers between LMVM and MVM. Three cytoskeletal proteins were probed by Western blotting in MVM and LMVM fractions. Ezrin β-actin and CK-7 are localized in different parts of the cytoskeletal microvilli (Berryman et al. 1995; Ikeda et al. 2006; Morales et al. 2004; Paku et al. 2005; Tyska et al. 2005; Wald et al. 2005). The first two are preferentially localized in the core of the finger-like projections, and their presence is significantly higher in MVM than in LMVM. By contrast, CK-7 is in the largest subfamily of intermediate filaments associated with syncytiotrophoblast cytoplasm (Paku et al. 2005), and its expression is enhanced in LMVM over MVM. These results could explain the presence of a second peak of PLAP and GM1 in the MVM flotation fractions, if the MVM microdomains are tightly associated with the specialized cytoskeleton of the finger-like projections region of the microvilli.

These findings support the possibility that MVM, LMVM and their respective rafts derive from two regions in the microvilli corresponding to subdomains of the apical hSTB membrane. As further support, previous functional studies of MVM and LMVM showed clear differences in the levels of diverse proteins, locating them in one of these two fractions (Bernucci et al, 2003; Berrios et al. 2008; Montalbetti et al. 2007; Riquelme et al. 1995, 2004; Riquelme and Parra 1999; Vallejos et al. 2008; Vallejos and Riquelme 2007). Our results are in agreement with a number of works that suggest similar heterogeneity for the apical domains (Danielsen and Hansen 2003). Hanono et al. (2006) proposed that microvilli contain subdomains distinguished by the localization of ezrin and EPI64.

In summary, our data support the presence of distinct lipid rafts in the two fractions of apical plasma membrane domains, both of which are insoluble in Triton X-100 and sensitive to cholesterol depletion. It seems plausible that MMV and LMVM apical fractions, with differences in cholesterol content and specific cytoskeletal proteins, correspond to specific regions of the microvillus and may explain the two types of raft we described. Figure 6 shows a possible model of MVM and LMVM localization in the microvilli of hSTB. In the apical domain of hSTB, the microvillous core composed of actin filaments is stabilized by actin cross-linked proteins such as ezrin. This specific region of finger-like projections might correspond to MVM, whose microdomains are strongly associated with its specialized cytoskeleton. LMVM, on the other hand,

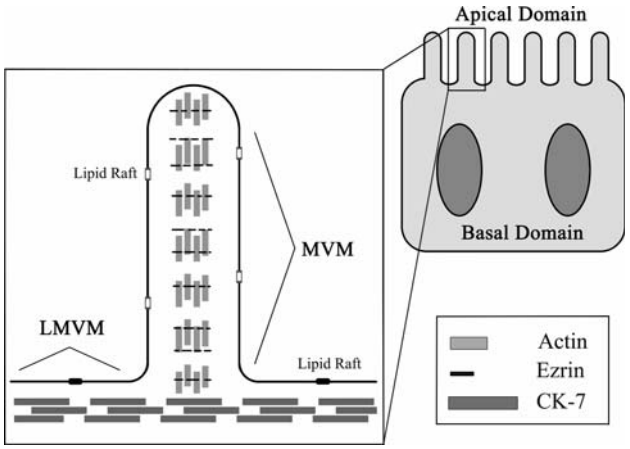

Fig. 6 Model of lipid raft localization in the microvilli of hSTB. Model proposes two distinct subdomains that could correspond to the purified apical membrane fractions. In white rectangles, lipid rafts of MVM could correspond to the finger-like projections of the microvilli, which are stabilized by their specific cytoskeleton. In black rectangles, rafts present in LMVM might correspond to the bottom part between the microvilli

could correspond to the bottom part of the microvilli, which is linked to distinct cytoskeletal proteins such as intermediate filament components (CK-7). Our data suggest that cytoskeletal factors are involved in the organization of apical rafts and that specific subdomain localization in the microvillus is the key to the differences between LMVM and MVM lipid raft composition. Finally, since many functions of the apical membrane are based on membrane dynamics and structure–function relationships, characterizing lipid rafts and the purified subdomains of the microvilli may be of great importance for understanding the molecular mechanisms of processes that occur in the placental hSTB. This model should be generally applicable to other types of epithelial cells. The next step in our work is to unravel the functional roles of these membrane microdomains in placental transport.

Acknowledgement We are grateful to Dr. M. Pérez and the staff at the San José Hospital Maternity Unit for assistance in obtaining the biological material. We also thank Dr. V. Illanes for critical reading of the manuscript and Mr. Aldo Valdebenito for technical assistance. This research was supported by grant Fondecyt–Chile 1070695.

References

Arvanitis DN, Min W, Gong Y, Heng YM, Boggs JM (2005) Two types of detergent-insoluble, glycosphingolipid/cholesterol-rich membrane domains from isolated myelin. J Neurochem 94: 1696–1710

Babiychuk EB, Draeger A (2000) Annexins in cell membrane dynamics. Ca^{2+}-regulated association of lipid microdomains. J Cell Biol 150:1113–1124

Babiychuk EB, Draeger A (2006) Biochemical characterization of detergent-resistant membranes: a systematic approach. Biochem J 397:407–416

Babiychuk EB, Monastyrskaya K, Burkhard FC, Wray S, Draeger A (2002) Modulating signaling events in smooth muscle: cleavage of annexin 2 abolishes its binding to lipid rafts. FASEB J 16:1177–1184

Bernucci L, Umana F, Llanos P, Riquelme G (2003) Large chloride channel from pre-eclamptic human placenta. Placenta 24:895–903

Berrios N, Diaz P, Riquelme G (2008) Functional incorporation of potassium channels from syncytiotrophoblast apical membrane into *Xenopus laevis* oocytes. Placenta 29:119

Berryman M, Gary R, Bretscher A (1995) Ezrin oligomers are major cytoskeletal components of placental microvilli: a proposal for their involvement in cortical morphogenesis. J Cell Biol 131:1231–1242

Braccia A, Villani M, Immerdal L, Niels-Christiansen LL, Nystrom BT, Hansen GH, Danielsen EM (2003) Microvillar membrane microdomains exist at physiological temperature. Role of galectin-4 as lipid raft stabilizer revealed by "superrafts". J Biol Chem 278:15679–15684

Brown DA, Rose JK (1992) Sorting of GPI-anchored proteins to glycolipid-enriched membrane subdomains during transport to the apical cell surface. Cell 68:533–544

Chatterjee S, Smith ER, Hanada K, Stevens VL, Mayor S (2001) GPI anchoring leads to sphingolipid-dependent retention of endocytosed proteins in the recycling endosomal compartment. EMBO J 20:1583–1592

Crane JM, Tamm LK (2004) Role of cholesterol in the formation and nature of lipid rafts in planar and spherical model membranes. Biophys J 86:2965–2979

Danielsen EM, Hansen GH (2003) Lipid rafts in epithelial brush borders: atypical membrane microdomains with specialized functions. Biochim Biophys Acta 1617:1–9

Delacour D, Jacob R (2006) Apical protein transport. Cell Mol Life Sci 63:2491–2505

Fantini J, Garmy N, Mahfoud R, Yahi N (2002) Lipid rafts: structure, function and role in HIV, Alzheimers and prion diseases. Expert Rev Mol Med 2002:1–22

Gaus K, Rodriguez M, Ruberu KR, Gelissen I, Sloane TM, Kritharides L, Jessup W (2005) Domain-specific lipid distribution in macrophage plasma membranes. J Lipid Res 46:1526–1538

Hanada K, Nishijima M, Akamatsu Y, Pagano RE (1995) Both sphingolipids and cholesterol participate in the detergent insolubility of alkaline phosphatase, a glycosylphosphatidylinositol-anchored protein, in mammalian membranes. J Biol Chem 270:6254–6260

Hanono A, Garbett D, Reczek D, Chambers DN, Bretscher A (2006) EPI64 regulates microvillar subdomains and structure. J Cell Biol 175:803–813

Harder T, Gerke V (1994) The annexin II2p11(2) complex is the major protein component of the triton X–100-insoluble low-density fraction prepared from MDCK cells in the presence of Ca^{2+}. Biochim Biophys Acta 1223:375–382

Harder T, Scheiffele P, Verkade P, Simons K (1998) Lipid domain structure of the plasma membrane revealed by patching of membrane components. J Cell Biol 141:929–942

Ikeda S, Fujimori M, Shibata S, Okajima M, Ishizaki Y, Kurihara T, Miyata Y, Iseki M, Shimizu Y, Tokumoto N, Ozaki S, Asahara T (2006) Combined immunohistochemistry of beta-catenin, cytokeratin 7, and cytokeratin 20 is useful in discriminating primary lung adenocarcinomas from metastatic colorectal cancer. BMC Cancer 6:31

Ikonen E (2001) Roles of lipid rafts in membrane transport. Curr Opin Cell Biol 13:470–477

Janich P, Corbeil D (2007) GM1 and GM3 gangliosides highlight distinct lipid microdomains within the apical domain of epithelial cells. FEBS Lett 581:1783–1787

Jimenez V, Henriquez M, Llanos P, Riquelme G (2004) Isolation and purification of human placental plasma membranes from normal and pre-eclamptic pregnancies: a comparative study. Placenta 25:422–437

Lagerholm BC, Weinreb GE, Jacobson K, Thompson NL (2005) Detecting microdomains in intact cell membranes. Annu Rev Phys Chem 56:309–336

Lichtenberg D, Goni FM, Heerklotz H (2005) Detergent-resistant membranes should not be identified with membrane rafts. Trends Biochem Sci 30:430–436

Llanos P, Henriquez M, Riquelme G (2002) A low conductance, non-selective cation channel from human placenta. Placenta 23:184–191

Macdonald JL, Pike LJ (2005) A simplified method for the preparation of detergent-free lipid rafts. J Lipid Res 46:1061–1067

Mazzone A, Tietz P, Jefferson J, Pagano R, LaRusso NF (2006) Isolation and characterization of lipid microdomains from apical and basolateral plasma membranes of rat hepatocytes. Hepatology 43:287–296

Meder D, Moreno MJ, Verkade P, Vaz WL, Simons K (2006) Phase coexistence and connectivity in the apical membrane of polarized epithelial cells. Proc Natl Acad Sci USA 103:329–334

Montalbetti N, Li Q, Wu Y, Chen XZ, Cantiello HF (2007) Polycystin–2 cation channel function in the human syncytiotrophoblast is regulated by microtubular structures. J Physiol 579:717–728

Morales FC, Takahashi Y, Kreimann EL, Georgescu MM (2004) Ezrin-radixin-moesin (ERM)-binding phosphoprotein 50 organizes ERM proteins at the apical membrane of polarized epithelia. Proc Natl Acad Sci USA 101:17705–17710

Nguyen HT, Amine AB, Lafitte D, Waheed AA, Nicoletti C, Villard C, Letisse M, Deyris V, Roziere M, Tchiakpe L, Danielle CD, Comeau L, Hiol A (2006) Proteomic characterization of lipid rafts markers from the rat intestinal brush border. Biochem Biophys Res Commun 342:236–244

Paku S, Dezso K, Kopper L, Nagy P (2005) Immunohistochemical analysis of cytokeratin 7 expression in resting and proliferating biliary structures of rat liver. Hepatology 42:863–870

Paradela A, Bravo SB, Henriquez M, Riquelme G, Gavilanes F, Gonzalez-Ros JM, Albar JP (2005) Proteomic analysis of apical microvillous membranes of syncytiotrophoblast cells reveals a high degree of similarity with lipid rafts. J Proteome Res 4:2435–2441

Pike LJ (2006) Rafts defined: a report on the Keystone symposium on lipid rafts and cell function. J Lipid Res 47:1597–1598

Rajendran L, Masilamani M, Solomon S, Tikkanen R, Stuermer CA, Plattner H, Illges H (2003) Asymmetric localization of flotillins/reggies in preassembled platforms confers inherent polarity to hematopoietic cells. Proc Natl Acad Sci USA 100:8241–8246

Rajendran L, Simons K (2005) Lipid rafts and membrane dynamics. J Cell Sci 118:1099–1102

Riquelme G, Parra M (1999) Regulation of human placental chloride channel by arachidonic acid and other cis unsaturated fatty acids. Am J Obstet Gynecol 180:469–475

Riquelme G, Stutzin A, Barros LF, Liberona JL (1995) A chloride channel from human placenta reconstituted into giant liposomes. Am J Obstet Gynecol 173:733–738

Riquelme G, Llanos P, Tischner E, Neil J, Campos B (2004) Annexin 6 modulates the maxi-chloride channel of the apical membrane of syncytiotrophoblast isolated from human placenta. J Biol Chem 279:50601–50608

Roper K, Corbeil D, Huttner WB (2000) Retention of prominin in microvilli reveals distinct cholesterol-based lipid micro-domains in the apical plasma membrane. Nat Cell Biol 2:582–592

Schroeder RJ, Ahmed SN, Zhu Y, London E, Brown DA (1998) Cholesterol and sphingolipid enhance the Triton X–100 insolubility of glycosylphosphatidylinositol-anchored proteins by promoting the formation of detergent-insoluble ordered membrane domains. J Biol Chem 273:1150–1157

Schuck S, Simons K (2004) Polarized sorting in epithelial cells: raft clustering and the biogenesis of the apical membrane. J Cell Sci 117:5955–5964

Simons K, Ehehalt R (2002) Cholesterol, lipid rafts, and disease. J Clin Invest 110:597–603

Simons K, Ikonen E (1997) Functional rafts in cell membranes. Nature 387:569–572

Simons K, Toomre D (2000) Lipid rafts and signal transduction. Nat Rev Mol Cell Biol 1:31–39

Smith PK, Krohn RI, Hermanson GT, Mallia AK, Gartner FH, Provenzano MD, Fujimoto EK, Goeke NM, Olson BJ, Klenk DC (1985) Measurement of protein using bicinchoninic acid. Anal Biochem 150:76–85

Taieb N, Yahi N, Fantini J (2004) Rafts and related glycosphingolipid-enriched microdomains in the intestinal epithelium: bacterial targets linked to nutrient absorption. Adv Drug Deliv Rev 56:779–794

Tyska MJ, Mackey AT, Huang JD, Copeland NG, Jenkins NA, Mooseker MS (2005) Myosin–1a is critical for normal brush border structure and composition. Mol Biol Cell 16:2443–2457

Vallejos C, Riquelme G (2007) The maxi-chloride channel in human syncytiotrophoblast: a pathway for taurine efflux in placental volume regulation? Placenta 28:1182–1191

Vallejos C, Guerrero I, Riquelme G (2008) Potassium channels in syncytiotrophoblast: an electrophysiological challenge. Placenta 29:123

van der Goot FG, Harder T (2001) Raft membrane domains: from a liquid-ordered membrane phase to a site of pathogen attack. Semin Immunol 13:89–97

Volonte D, Galbiati F, Li S, Nishiyama K, Okamoto T, Lisanti MP (1999) Flotillins/cavatellins are differentially expressed in cells and tissues and form a hetero-oligomeric complex with caveolins in vivo. Characterization and epitope-mapping of a novel flotillin–1 monoclonal antibody probe. J Biol Chem 274:12702–12709

Wald FA, Oriolo AS, Casanova ML, Salas PJ (2005) Intermediate filaments interact with dormant ezrin in intestinal epithelial cells. Mol Biol Cell 16:4096–4107

Wiechelman KJ, Braun RD, Fitzpatrick JD (1988) Investigation of the bicinchoninic acid protein assay: identification of the groups responsible for color formation. Anal Biochem 175:231–237

Xu W, Yoon SI, Huang P, Wang Y, Chen C, Chong PL, Liu-Chen LY (2006) Localization of the kappa opioid receptor in lipid rafts. J Pharmacol Exp Ther 317:1295–1306